



**HAL**  
open science

# Comparison of noise-magnitude and noise-texture across two generations of iterative reconstruction algorithms from three manufacturers

J. Frandon, G. Moliner, J.P. Beregi, F. Pereira, J. Greffier, A. Larbi

► **To cite this version:**

J. Frandon, G. Moliner, J.P. Beregi, F. Pereira, J. Greffier, et al.. Comparison of noise-magnitude and noise-texture across two generations of iterative reconstruction algorithms from three manufacturers. *Diagnostic and Interventional Imaging*, 2019, 100 (7-8), pp.401–410. 10.1016/j.diii.2019.04.006 . hal-02931820

**HAL Id: hal-02931820**

**<https://hal.umontpellier.fr/hal-02931820>**

Submitted on 25 Oct 2021

**HAL** is a multi-disciplinary open access archive for the deposit and dissemination of scientific research documents, whether they are published or not. The documents may come from teaching and research institutions in France or abroad, or from public or private research centers.

L'archive ouverte pluridisciplinaire **HAL**, est destinée au dépôt et à la diffusion de documents scientifiques de niveau recherche, publiés ou non, émanant des établissements d'enseignement et de recherche français ou étrangers, des laboratoires publics ou privés.



Distributed under a Creative Commons Attribution - NonCommercial 4.0 International License

# **Comparison of noise-magnitude and noise-texture across two generations of iterative reconstruction algorithms from three manufacturers**

J. Greffier<sup>\*</sup>, A. Larbi, J. Frandon, G. Moliner, J.P. Beregi, F. Pereira

Department of Radiology, CHU Nîmes, Univ Montpellier, Medical Imaging Group Nîmes,  
30029 Nîmes, France

\* Corresponding author: [joel.greffier@chu-nimes.fr](mailto:joel.greffier@chu-nimes.fr)

CHU de Nîmes, Medical Imaging Group Nîmes, EA 2415, Bd Prof Robert Debré, 30029  
Nîmes Cedex 9, france

## Abstract

**Purpose:** To compare the noise-magnitude and noise-texture across two generations of iterative reconstruction (IR) algorithms proposed by three manufacturers according to the dose level.

**Materials and Methods:** Five computed tomography (CT) systems equipped with two generations of IR algorithm (hybrid/statistical IR [H/SIR] or full/partial model-based IR [MBIR]) were compared. Acquisitions on Catphan 600 phantom were performed at 120 kV and three dose levels (3-, 7- and 12-mGy). Raw data were reconstructed using standard “soft tissue” kernel for filtered back projection and one iterative level of two generations of IR algorithms. Contrast to-noise-ratio (CNR) was computed using three regions of interest: two of them placed in the low-density polyethylene (LDPE) and Teflon<sup>®</sup> inserts and another placed on the solid water. Noise power spectrum (NPS) was computed to assess the noise-magnitude (NPS-peak) and noise-texture (NPS spatial frequency).

**Results:** CNR increased significantly in MBIR compared to H/SIR algorithms for General-Electric (GE) Healthcare ( $45\% \pm 12$  [SD]) and Philips Healthcare systems ( $62\% \pm 11$  [SD]) ( $P < 0.001$ ). Regarding Siemens Healthineers systems, CNR of MBIR was significantly lower than that of H/SIR (mean difference:  $-4\% \pm 5$  [SD]) ( $P < 0.001$ ) for Teflon<sup>®</sup> insert but not for LDPE insert (mean difference:  $-4\% \pm 7$  [SD]) ( $P = \text{NS}$ ). NPS peaks were lower with MBIR than with H/SIR for GE Healthcare ( $-42\% \pm 8$  [SD]) and Philips Healthcare ( $-75\% \pm 4$  [SD]) systems, whereas it was greater with MBIR than with H/SIR for Siemens Healthineers ( $13\% \pm 11$  [SD]) systems. NPS spatial frequencies were higher with MBIR than with H/SIR for Siemens ( $14\% \pm 10$  [SD]) but lower for others ( $-17\% \pm 5$  [SD] for GE Healthineers and  $-55\% \pm 3$  [SD] for Philips Healthcare systems).

**Conclusion:** This study demonstrates that recent MBIR algorithms, by comparison with the preceding generation, differ according to the main manufacturers with respect to noise-magnitude and noise-texture.

**Keywords:** Multidetector computed tomography; Image quality enhancement; Iterative reconstruction; optimization; Noise power spectrum

## Abbreviations

CNR: Contrast-to-noise ratio

CT: Computed tomography

FBP: Filtered back projection

GE: General Electric

H/SIR: Hybrid/statistical Iterative reconstruction

IR: Iterative reconstruction

MBIR: Model-based iterative reconstruction

NPS: Noise power spectrum

ROI: Region of interest

## **Introduction**

The increasing number of computed tomography (CT) examinations performed each year has led to a major public health concern due to the increased risk of collective radiation dose [1]. To reduce the delivered dose, an optimization of practice and procedures is essential [2; 3]. This task is complex, as radiation dose has a direct influence on image quality and any attempt to reduce the dose delivered must ensure that image quality remains adequate for a reliable diagnosis [2; 3].

The two-dimensional (2D) projection images acquired from the CT scanners are processed through various reconstruction algorithms to obtain the 3D/volumetric images such as iterative reconstruction (IR) algorithms. IR algorithm has a twofold interest [4-8]. First, for the same delivered dose, IR algorithm improves image quality without changing the mean attenuation or the modulation transfer function, which is commonly used to estimate the spatial transverse resolution. Second, IR allows dose reduction whilst maintaining the image quality indexes. However, these algorithms present non-linearity and non-stationary properties that change the noise texture, leading to changes in image quality assessment [9]. To date, usual image quality indexes, such as image noise and contrast-to noise ratio) are not sufficient to objectively evaluate the image quality with IR algorithms. This evaluation must be conducted using new metrics such as the noise power spectrum (NPS). As defined by Verdun et al., NPS gives a complete description of the noise by plotting the amplitude (noise-magnitude) according to the frequency of the image, which is known as noise-texture (*e.g.*, image smoothing) [9].

Several generations of IR algorithm are proposed by CT system manufacturers [10; 11]. The most common IR algorithms are hybrid or statistical IR (H/SIR) algorithms that combine filtered back projection (FBP) and IRs in different proportions. For some systems, this proportion can be selected by the user, such as adaptive statistical iterative reconstruction (ASIR, General Electric [GE] Healthcare). Another recent algorithm is the model-based iterative reconstructions (MBIR) that generates CT reconstructions via a probabilistic method, deriving a statistical cost function through incorporation of X-ray physics and CT optics modeling to effectively reduce noise and artifacts and even enhance spatial resolution [12; 13]. The reconstruction time with full MBIR algorithm (Veo<sup>®</sup>, GE Healthcare) is relatively long and manufacturers also propose a fast partial version [11].

Few studies have compared differences in the noise-magnitude and noise-texture for hybrid/statistical and partial/full-MBIR algorithms proposed by four manufacturers. Some authors have compared the performance of H/SIR or MBIR algorithms by the same manufacturer [14; 15], while others have evaluated the impact of one IR algorithm of each manufacturer compared to the FBP [16; 17].

The aim of this study was to evaluate the noise-magnitude and the noise-texture produced by two generations of IR algorithms of three manufacturers.

## **Materials and methods**

### *CT systems*

Five CT systems from different brands were used for this study: Revolution GSI<sup>®</sup> (GE Healthcare), Revolution Evo<sup>®</sup> (GE Healthcare), Ingenuity Elite<sup>®</sup> (Philips Healthcare), Somatom Definition AS+<sup>®</sup> (Siemens Healthineers) and Somatom EDGE<sup>®</sup> (Siemens Healthineers). Acquisitions on Revolution EVO<sup>®</sup>, Somatom EDGE<sup>®</sup> and Ingenuity Elite<sup>®</sup> units were performed outside of our institution. The other acquisitions were performed on two CT units of our institution.

### *Experiment procedure*

A Catphan 600 phantom (The Phantom Laboratory) was scanned in a helical mode with a pitch factor close to 1 (Fig. 1a). The tube voltage was 120 kV and the tube currents (mA) were defined to obtain three different dose levels: 3.0, 7.0 and 12.0mGy. These dose levels correspond to the usually delivered dose in our institution for thoracic, abdominal-pelvic and

lumbar spine acquisitions, respectively. All acquisitions were performed with a rotation time of 0.5 s/rotation and tube current modulation was disabled.

To reduce the amount of data analyzed in this paper, raw data were only reconstructed with standard “soft tissue” reconstruction kernel and with the FBP and the intermediate iterative level of the two generations of IR algorithm (H/SIR and MBIR algorithms) available on each system and usually used in clinical practice. IR level and kernel for each CT system were defined with support of the application engineer of each manufacturer. Acquisitions with Siemens Healthineers and GE Healthcare systems were performed on two different CT units. Both Siemens Healthineers systems were equipped with different detectors.

Images were reconstructed with a field-of-view of 250 mm and a slice thickness close to 1 mm (1 mm increment). All acquisition and reconstruction parameters used in this study are shown in Table 1.

### *Dosimetry*

The volume CT dose indexes (CTDI<sub>vol</sub>), determined for a 32 cm-diameter (polymethyl methacrylate) reference phantom were retrieved from the reports available in the CT workstation at the end of the acquisitions.

### *Contrast-to-noise ratio (CNR)*

Image quality evaluations were performed using in-house Matlab (MathWorks, Natick, USA) routines. Two circular regions of interest (ROI) of 420 pixels (0.785 cm<sup>2</sup>) were placed on the CTP 401 section in two inserts: Teflon<sup>®</sup> (range from 941 to 1060HU) and LDPE (range from -121 to -87HU). The N<sub>CT</sub> and the image noise of the solid water (range from -7 to 7HU) on the CTP 486 section were assessed by placing a ROI of 14,400 pixels (36 cm<sup>2</sup>) in the center of the phantom (Fig. 1b). The CT number (average of pixels) and image-noise (standard deviation of pixels) were computed within each ROI in 15 consecutive reconstructed slices [14].

The contrast-to-noise ratio between both inserts and the solid water was calculated as follows:

$$CNR = \frac{|HU_{Insert} - HU_{Water}|}{\sigma_{Water}}$$

where HU indicates Hounsfield unit.

### *Noise power spectrum*

NPS were calculated with a homemade MATLAB<sup>®</sup> routine (The MathWorks, Natick, USA) in the uniform section of Catphan phantom (CTP 406) as follows:

$$NPS_{2D}(f_x, f_y) = \frac{\Delta_x \Delta_y}{L_x L_y} \frac{1}{N_{ROI}} \sum_{i=1}^{N_{ROI}} \left| TFD_{2D} \{ ROI_i(x, y) - \overline{ROI_i} \} \right|^2,$$

where  $\Delta_x$  and  $\Delta_y$  are the pixel size in x- and y-direction;  $L_x$  et  $L_y$  are the ROIs length in the x- and y-directions;  $N_{ROI}$  the number of ROI and  $\overline{ROI_i}$  is the background or structured noise measured from ROI (x, y) using a first-order (subtraction of a 3D linear fit) detrending technique.

NPS was computed in a total of 80 ROIs, 64×64 pixels each, within 20 consecutive axial sections (Fig. 1c).

### *Visual assessment of image quality*

In order to illustrate the differences between H/SIR and MBIR algorithms for noise-magnitude and noise-texture, a 4×4 cm<sup>2</sup> image was extracted from the center of the uniform section. The window and level were fixed to 370 HU and 60 HU, respectively.

### *Statistical analysis*

Statistical analyses were performed out using our in-house developed MATLAB routine (MathWorks, Natick, USA). Quantitative variables were expressed as medians, first (Q<sub>1</sub>) and third (Q<sub>3</sub>) quartiles. Comparisons of CNR values between FBP and algorithms were performed using the Wilcoxon rank sum test. *P* values were corrected for multiple comparisons (Bonferonni test) and only values lower than 0.001 (*P* corrected < 0.001) were considered to indicate significance due to multiple comparisons.

## Results

### *Contrast-to-noise ratio*

The CNR values for reconstructions with FBP, H/SIR and MBIR as function of the dose levels are shown in Figure 2 and Table 2 for both inserts. CNR for FBP was lower than H/SIR or MBIR algorithms. These differences were significant for all CT scanners and insert ( $P < 0.001$ ). On average, CNR improved from FBP to H/SIR algorithms about  $44\% \pm 1$  (SD) for GE Healthcare,  $28\% \pm 1$  (SD) for Philips Healthcare and  $48\% \pm 1$  (SD) for Siemens Healthineers systems. In both inserts, CNR were significantly higher in FBP-Evo than FBP-GSI ( $P < 0.001$ ). Regarding Siemens Healthineers systems, CNR values were significantly greater in FBP-Edge than FBP-AS+ for Teflon<sup>®</sup> insert but not significant for LDPE insert ( $P=0.003$  for 3 mGy;  $P=0.002$  for 7 mGy and  $P=0.472$  for 12mGy). On average, CNR was improved by  $7\% \pm 1$  (SD) for GE Healthcare and  $7\% \pm 6$  (SD) for Siemens Healthineers systems.

Regarding GE Healthcare systems (Figs. 2a and 2.b), CNR was significantly greater with "Asir-V 50%" than with "Asir 50%" for all dose levels and for both insert ( $P < 0.001$ ). On average, CNR improved from "Asir" to "Asir-V" about  $44\% \pm 13$  (SD) for Teflon<sup>®</sup> insert and  $47\% \pm 13$  (SD) for LDPE insert. Moreover, differences between both IR algorithms decreased with the dose level (e.g. 60% for 12mGy, 45% for 7mGy and 35% for 3mGy with LDPE insert).

With respect to Philips Healthcare system (Figs. 2c and 2d), "IMR 2" resulted in significantly greater CNR values than "iDose<sup>4</sup> 3" for both inserts ( $P < 0.001$ ). The mean CNR improved from "iDose<sup>4</sup>" to "IMR" of  $62\% \pm 11$ (SD) for Teflon<sup>®</sup> insert and  $63\% \pm 11$  (SD) for LDPE insert. Like GE healthineers systems, differences between both IR algorithms decreased with the dose level (e.g., 78% for 12mGy, 57% for 7mGy and 51% for 3mGy with Teflon<sup>®</sup> insert).

Regarding Siemens Healthineers systems (Figs. 2.e and 2.f), CNR were significantly lower in "ADMIRE 3" than "SAFIRE 3" ( $P < 0.001$ ) for Teflon<sup>®</sup> insert but not significantly lower for LDPE insert ( $P=0.003$  for 3 mGy;  $P=0.005$  for 7 mGy and  $P=0.002$  for 12mGy). On average, CNR was decreased from "ADMIRE 3" to "SAFIRE 3" of  $-4\% \pm 5$  (SD) for Teflon<sup>®</sup> insert and  $-4\% \pm 7\%$  (SD) for LDPE insert.



## *Noise power spectrum*

### **NPS-peak**

Independently of the system and the reconstruction algorithms, NPS peaks decreased as the dose increased (Table 3) (Fig. 3).

NPS peak with FBP was greater than with H/SIR or MBIR algorithms. The mean NPS peak decreased from FBP to H/SIR algorithms of  $-33\% \pm 1$  (SD) for GE Healthcare,  $-31\% \pm 2$  (SD) for Philips Healthcare and  $-46\% \pm 3$  (SD) for Siemens Healthineers systems. NPS peak were lower in FBP-Edge than FBP-AS+ and in FBP-Evo than FBP-GSI. On average NPS peak was decreased by  $-11\% \pm 2$  (SD) for GE Healthcare and  $-8\% \pm 7$  (SD) for Siemens Healthineers systems.

Regarding GE Healthcare systems (Fig. 3a), NPS peak were lower in “Asir-V 50%” than in “Asir 50%” ( $-42\% \pm 8$  [SD]) for all dose levels (Table 3). Moreover, differences between both IR algorithms decreased with the dose level (*e.g.*,  $-51\%$  for 3 mGy,  $-41\%$  for 7 mGy and  $34\%$  for 12 mGy). A similar pattern was found for Philips Healthcare system (Fig. 3b), although differences between “IMR 2” and iDose<sup>4</sup> 3” were even more pronounced ( $-75\% \pm 4$  [SD]). With respect to Siemens Healthineers systems (Fig. 3c), weighted NPS peaks of “ADMIRE 3” were an average of  $13\% \pm 11$  (SD) greater than “SAFIRE 3”. These differences between both IR algorithms increased with the dose level (*e.g.*,  $1\%$  for 3mGy,  $15\%$  for 7mGy and  $22\%$  for 12mGy).

### **Noise-texture**

NPS spatial frequencies of IR algorithms were lower than FBP for all systems (Table 3) (Fig. 4). Differences between H/SIR and FBP were  $-6\% \pm 2$  (SD) for Philips,  $-27\% \pm 1$  (SD) for GE Healthcare and  $-55\% \pm 3$  (SD) for Siemens Healthcare systems. Similar NPS spatial frequency values were found for both FBP with GE Healthcare ( $0.298\text{mm}^{-1} \pm 0.010$ ) and with Siemens Healthineers ( $0.210 \text{mm}^{-1} \pm 0.011$  [SD]) systems.

NPS spatial frequencies of MBIR were lower than H/SIR algorithms for GE Healthcare and Philips Healthcare systems (Table 3) (Fig. 4). Differences between MBIR and H/SIR were on average:  $-17\% \pm 5$  (SD) and  $-55\% \pm 3$ (SD), respectively. However, the opposite was found for Siemens Healthineers systems (Fig. 4c). NPS spatial frequencies of MBIR were on average  $14\% \pm 10$  (SD) greater than IR. For MBIR algorithms, lowest values of NPS spatial frequency were found for Philips Healthcare system ( $0.087\text{mm}^{-1} \pm 0.006$  [SD]).

## *Visual assessment of image quality*

Figure 4 illustrate qualitatively the noise-magnitude and noise-texture for all H/SIR and MBIR algorithms. The noise-magnitude appears greater in the H/SIR images than MBIR. This parameter was visually more evident for Philips Healthcare system whereas it was moderate or less evident for GE Healthcare and Siemens Healthineers systems. Similar patterns were found for noise-texture.

## **Discussion**

Experimental and clinical studies have established that IR is an important tool to reduce CT radiation doses [4-8]. However, when evaluating images reconstructed with IR algorithms, some criteria must be taken into account such as the noise characteristics. The impact of IR on noise-texture and noise-magnitude was dependent of the generation of IR algorithms employed and the CT manufacturer. For the first time, the present study evaluated the noise-magnitude and noise-texture for both generations of algorithm, proposed by GE Healthcare, Philips Healthcare and Siemens Healthineers systems.

Our results are consistent with those of previous studies [14, 15, 17, 20, 21]. CNR values improved when the dose increased but also with both generations of IR algorithms regarding the FBP[14]. Comparison between H/SIR and MBIR reveal that CNR values were improved in GE Healthcare and Philips Healthcare systems, respectively. For the latter, a similar outcome was previously presented by Aurumskjöld *et al.* using an anthropomorphic phantom [15]. Opposite pattern was found for Siemens Healthineers system. Indeed, CNR values were lower with ADMIRE than with SAFIRE. It should also be noted that CNR values using FBP were different for both General Electric Healthcare systems and the two Siemens Healthineers systems evaluated. Both Siemens Heathineers systems were equipped with different detectors.

Our results confirm those of previous studies showing that NPS peak and NPS spatial frequency decreased in both generations of IR algorithms when compared to the FBP [14, 15, 17-19, 21-24]. In addition, direct comparison between H/SIR and MBIR algorithms demonstrated opposite features between manufacturers. For instance, the noise-magnitude in GE Healthcare and Philips Healthcare systems reduced from H/SIR to MBIR algorithms whereas it increased for Siemens Healthineers system. This reversion pattern was also found for noise-texture. Siemens Healthineers systems shifted toward high frequencies whereas it displaced toward low frequencies for the other manufacturers, especially for Philips

Healthcare system. For the latter, similar outcomes were found by Paruccini et al. with a 20 cm diameter phantom [24] and by Aurumskjöld et al. using an anthropomorphic phantom [15]. Regarding the other manufacturers, few studies compared H/SIR and MBIR algorithms under the same conditions (*e.g.*, phantom type and size, iterative level). However, we found similar results for NPS curves, being in the range of those previously described for GE Healthcare [14; 18] and Siemens Healthineers [21; 25] systems.

For GE Healthcare systems, images appear with less noise and more smoothness in MBIR than H/SIR. A similar outcome was found by Samei et al. with Asir 50% and Veo algorithms [14]. Similar features to GE Healthcare systems were also found for Philips Healthcare system. However, the reduction of image noise is more important using MBIR faced to H/SIR and the images are more smoothed than with GE Healthcare systems. As far as the images are smoothed radiologist will face more difficulties to interpret the images. Regarding Siemens Healthineers systems, noise and smoothness appear similar for both algorithms.

This study has some limitations. First, raw-data were reconstructed using a single kernel and one iterative level. Such combination of parameters is an example of multiple combinations that can produced different results. Second, the effect of the two generations of IR algorithm on spatial resolution (*e.g.*, Target transfer function) and on detectability indexes ( $d'$ ) was not performed [9, 14, 25, 26]. These limitations did not affect the interpretation of the study, which aimed to focus on the two generations of IR algorithms of each manufacturer. For GE Healthcare and Siemens Healthineers systems, the assessment of noise-texture and noise-magnitude was performed on two different CT systems with different geometry and detectors. Finally, since this study was performed with a single phantom, the outcome could be different in a patient study.

In conclusion, this phantom study performed with a soft reconstruction kernel and an intermediate iterative level suggested that features of the recent MBIR algorithms compared to the preceding generation differ according to the main manufacturers. For instance, GE Healthcare and Philips Healthcare systems reduce the noise-magnitude in detriment to the image smoothness. Siemens Healthineers systems keep noise-magnitude approximately the same but images were less smoothed.

## **Conflicts of interest**

None of the authors have conflict of interest or industry support of the project to declare.

## **Acknowledgements**

We would like to thank Dr J.M. Teissier for giving us permission to use the results of these measurements. We thank F. Mahinc and D. OM for their support in this study. We thank S. Kabani for her help in editing the manuscript. We thank C. Demattei for his statistical support.

## REFERENCES

- 1 Brenner DJ, Hall EJ. Computed tomography: an increasing source of radiation exposure. *N Engl J Med* 2007; 357:2277-84.
- 2 Kalra MK, Maher MM, Toth TL, Hamberg LM, Blake MA, Shepard JA, et al. Strategies for CT radiation dose optimization. *Radiology* 2004; 230:619-28.
- 3 Gunn ML, Kohr JR. State of the art: technologies for computed tomography dose reduction. *Emerg Radiol* 2010; 17:209-18.
- 4 Larbi A, Orliac C, Frandon J, Pereira F, Ruyer A, Goupil J, et al. Detection and characterization of focal liver lesions with ultra-low dose computed tomography in neoplastic patients. *Diagn Interv Imaging* 2018; 99:311-20.
- 5 Macri F, Greffier J, Pereira F, Rosa AC, Khasanova E, Claret PG, et al. Value of ultra-low-dose chest CT with iterative reconstruction for selected emergency room patients with acute dyspnea. *Eur J Radiol* 2016; 85:1637-44.
- 6 Yamada Y, Jinzaki M, Hosokawa T, Tanami Y, Sugiura H, Abe T, et al. Dose reduction in chest CT: comparison of the adaptive iterative dose reduction 3D, adaptive iterative dose reduction, and filtered back projection reconstruction techniques. *Eur J Radiol* 2012; 81:4185-95.
- 7 Katsura M, Matsuda I, Akahane M, Sato J, Akai H, Yasaka K, et al. Model-based iterative reconstruction technique for radiation dose reduction in chest CT: comparison with the adaptive statistical iterative reconstruction technique. *Eur Radiol* 2012; 22:1613-23.
- 8 Yan C, Xu J, Liang C, Wei Q, Wu Y, Xiong W, et al. Radiation dose reduction by using CT with iterative model reconstruction in patients with pulmonary invasive fungal infection. *Radiology* 2018; 288:285-92.
- 9 Verdun FR, Racine D, Ott JG, Tapiovaara MJ, Toroi P, Bochud FO, et al. Image quality in CT: from physical measurements to model observers. *Phys Med* 2015; 31:823-43.
- 10 Patino M, Fuentes JM, Hayano K, Kambadakone AR, Uyeda JW, Sahani DV. A quantitative comparison of noise reduction across five commercial (hybrid and model-based) iterative reconstruction techniques: an anthropomorphic phantom study. *AJR Am J Roentgenol* 2015; 204:W176-83.
- 11 Viry A, Aberle C, Racine D, Knebel JF, Schindera ST, Schmidt S, et al. Effects of various generations of iterative CT reconstruction algorithms on low-contrast

detectability as a function of the effective abdominal diameter: a quantitative task-based phantom study. *Phys Med* 2018; 48:111-8.

12 McCollough CH, Chen GH, Kalender W, Leng S, Samei E, Taguchi K, et al. Achieving routine submillisievert CT scanning: report from the summit on management of radiation dose in CT. *Radiology* 2012; 264:567-80.

13 Thibault JB, Sauer KD, Bouman CA, Hsieh J. A three-dimensional statistical approach to improved image quality for multislice helical CT. *Med Phys* 2007; 34:4526-44.

14 Samei E, Richard S. Assessment of the dose reduction potential of a model-based iterative reconstruction algorithm using a task-based performance metrology. *Med Phys* 2015; 42:314-23.

15 Aurumskjold ML, Ydstrom K, Tingberg A, Soderberg M. Improvements to image quality using hybrid and model-based iterative reconstructions: a phantom study. *Acta Radiol* 2017; 58:53-61.

16 Love A, Olsson ML, Siemund R, Stalhammar F, Bjorkman-Burtscher IM, Soderberg M. Six iterative reconstruction algorithms in brain CT: a phantom study on image quality at different radiation dose levels. *Br J Radiol* 2013; 86:20130388.

17 Christianson O, Chen JJ, Yang Z, Saiprasad G, Dima A, Filliben JJ, et al. An improved index of image quality for task-based performance of CT iterative reconstruction across three commercial implementations. *Radiology* 2015; 275:725-34.

18 Euler A, Solomon J, Marin D, Nelson RC, Samei E. A third-generation adaptive statistical iterative reconstruction technique: phantom study of Image Noise, Spatial Resolution, Lesion Detectability, and Dose Reduction Potential. *AJR Am J Roentgenol* 2018; 210:1301-8.

19 Morsbach F, Desbiolles L, Raupach R, Leschka S, Schmidt B, Alkadhi H. Noise texture deviation: a measure for quantifying artifacts in computed tomography images with Iterative reconstructions. *Invest Radiol* 2017; 52:87-94.

20 Greffier J, Macri F, Larbi A, Fernandez A, Khasanova E, Pereira F, et al. Dose reduction with iterative reconstruction: optimization of CT protocols in clinical practice. *Diagn Interv Imaging*. 2015; 96:477-86.

21 Greffier J, Macri F, Larbi A, Fernandez A, Pereira F, Mekkaoui C, et al. Dose reduction with iterative reconstruction in multi-detector CT: What is the impact on

deformation of circular structures in phantom study? *Diagn Interv Imaging* 2016; 97:187-96.

22 Solomon J, Mileto A, Ramirez-Giraldo JC, Samei E. Diagnostic performance of an advanced modeled Iterative reconstruction algorithm for low-contrast detectability with a third-generation dual-source multidetector CT scanner: potential for radiation dose Reduction in a Multireader Study. *Radiology* 2015; 275:735-45.

23 De Marco P, Origgi D. New adaptive statistical iterative reconstruction ASiR-V: Assessment of noise performance in comparison to ASiR. *J Appl Clin Med Phys* 2018; 19:275-86.

24 Paruccini N, Villa R, Pasquali C, Spadavecchia C, Baglivi A, Crespi A. Evaluation of a commercial model based iterative reconstruction algorithm in computed tomography. *Phys Med* 2017;41:58-70.

25 Solomon JB, Christianson O, Samei E. Quantitative comparison of noise texture across CT scanners from different manufacturers. *Med Phys* 2012; 39:6048-55.

26 Ott JG, Becce F, Monnin P, Schmidt S, Bochud FO, Verdun FR. Update on the non-prewhitening model observer in computed tomography for the assessment of the adaptive statistical and model-based iterative reconstruction algorithms. *Phys Med Biol* 2014; 59:4047-64.

## Figure legends

**Figure 1.** Figure shows the different regions of interest (ROI) used in this study. a. ROIs used to compute the  $N_{CT}$  and image noise of Teflon® insert and low-density polyethylene (LDPE) insert (2.), b. ROI used to compute the  $N_{CT}$  and image noise of solid water and c. ROIs used to the noise power spectrum assessment.

**Figure 2.** Column bars show the mean values of contrast-to-noise ratio for Teflon® (A, C, E) and low-density polyethylene (LDPE) (B, D, F) inserts as function of the dose levels (CTDIvol in mGy) for filtered back projection (FBP), hybrid/statistical iterative reconstruction (H/SIR) and model-based iterative reconstruction (MBIR) algorithms of three manufacturers. GE indicates General Electric Healthcare; Philips indicates Philips Healthcare. Siemens indicates Siemens Healthineers.

**Figure 3.** Diagrams show noise power spectrum (NPS) curves weighted by NPS peak of filtered back projection (FBP) at each dose level (3, 7 and 12 mGy) for hybrid/statistical iterative reconstruction (H/SIR) and model-based iterative reconstruction (MBIR) algorithms of three manufacturers. GE indicates General Electric Healthcare; Philips indicates Philips Healthcare. Siemens indicates Siemens Healthineers.

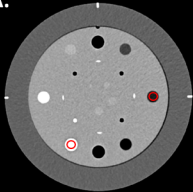
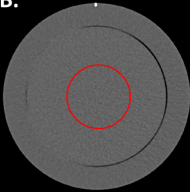
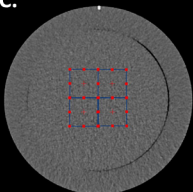
**Figure 4.** Image quality in region of interest (ROI) of  $4 \times 4 \text{cm}^2$  placed into the uniform section of the Catphan 600 phantom for hybrid/statistical iterative reconstruction (H/SIR) and model-based iterative reconstruction (MBIR) algorithms of three manufacturers as a function of the dose level (3, 7 and 12 mGy). GE indicates General Electric Healthcare; Philips indicates Philips Healthcare. Siemens indicates Siemens Healthineers.

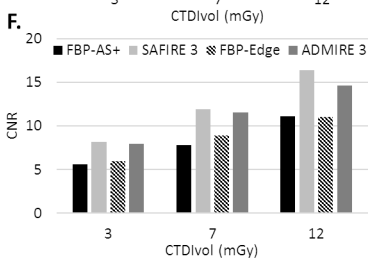
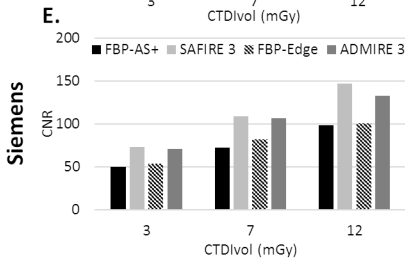
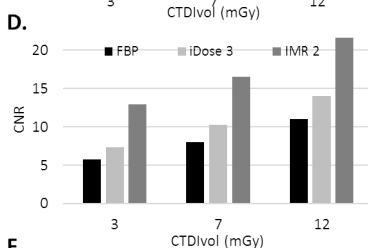
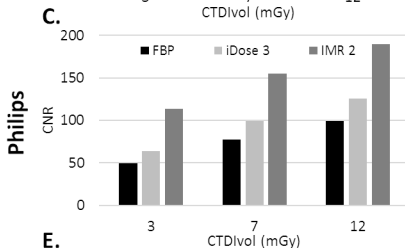
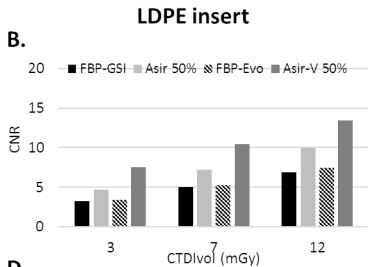
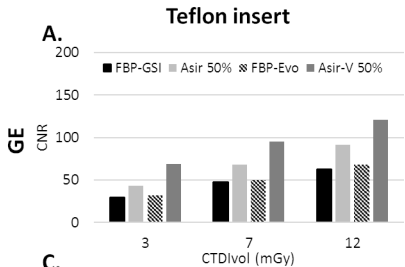
**Table 1.** Acquisition and reconstruction parameters used on each CT scanner unit.

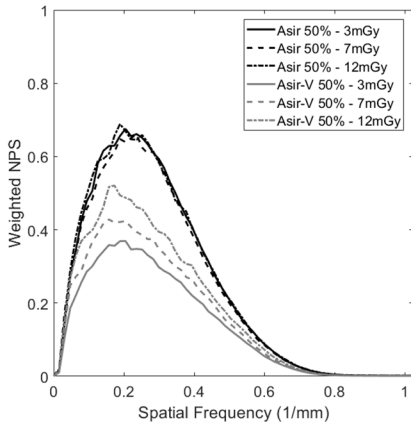
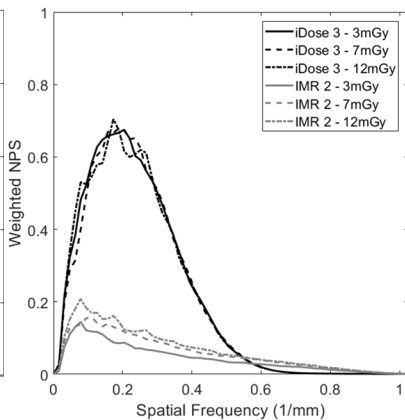
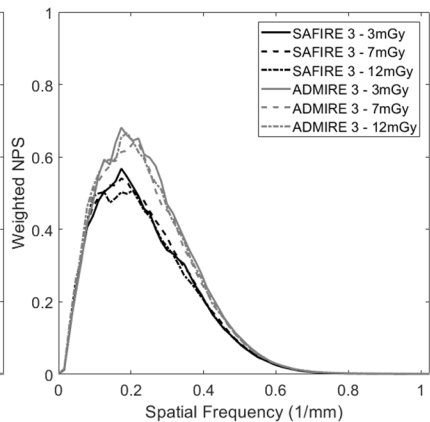
**Table 2.** Contrast to noise ratio (CNR) of Teflon® and low-density polyethylene (LDPE) inserts obtained with soft kernels according to the dose level for each CT scanner unit and reconstruction type.

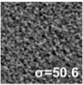
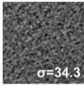
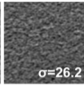
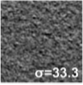
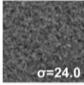
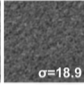
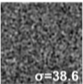
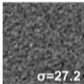
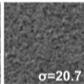
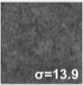
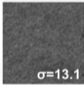
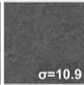
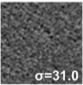
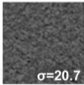
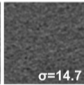
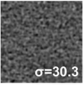
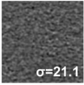
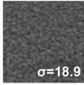
**Table 3.** Noise power spectrum (NPS) peak and spatial frequency according to the dose level for each CT unit and reconstruction type.



**A.****B.****C.**



**A.****GE****B.****Philips****C.****Siemens**

		3 mGy	7 mGy	12 mGy
<b>GE</b>	<b>Asir 60%</b>	 $\sigma=50.6$	 $\sigma=34.3$	 $\sigma=26.2$
	<b>Asir-V 60%</b>	 $\sigma=33.3$	 $\sigma=24.0$	 $\sigma=18.9$
<b>Philips</b>	<b>iDose 4</b>	 $\sigma=38.6$	 $\sigma=27.2$	 $\sigma=20.7$
	<b>IMR 2</b>	 $\sigma=13.9$	 $\sigma=13.1$	 $\sigma=10.9$
<b>Siemens</b>	<b>SAFIRE 3</b>	 $\sigma=31.0$	 $\sigma=20.7$	 $\sigma=14.7$
	<b>ADMIRE 3</b>	 $\sigma=30.3$	 $\sigma=21.1$	 $\sigma=18.9$

Manufacturer	GE Healthcare		Philips Healthcare	Siemens Healthineers		
Model	Revolution® GSI	Revolution® Evo	Ingenuity® Elite	Definition® AS+	EDGE®	
mAs values used according to the CTDIvol	12 mGy	290	270	184	178	178
	7 mGy	170	160	107	104	104
	3 mGy	70	70	46	45	45
Pitch	0.984		0.984	1	1	
IR algorithm and IR level	Asir 50%	Asir-V 50%	iDose <sup>4</sup> 3 / IMR 2	SAFIRE 3	ADMIRE 3	
Reconstruction kernel	Standard	Standard	A / Routine	I30f	I30f	
Detector	Gemstone	Gemstone	Elite IMR Ready	Ultra Fast Ceramic	Stellar	
Thickness/Overlapped	1.25mm/1.25mm		1mm/1mm	1mm/1mm		
Collimation	64x0.625 mm		64x0.625 mm	64x0.6 mm		

Note. CTDIvol indicates volume CT dose index; IR indicates iterative reconstruction. ASIR indicates adaptive statistical iterative reconstruction.

Manufacturer	Reconstruction type	CNR Teflon <sup>®</sup>			CNR LDPE		
		3 mGy	7 mGy	12 mGy	3 mGy	7 mGy	12 mGy
GE Healthcare	FBP-GSI	29.9 (29.6; 30.1)	47.6 (47.4; 47.7)	62.7 (62.5; 62.8)	3.3 (3.2; 3.4)	5.1 (5.0; 5.2)	6.8 (6.8; 6.9)
	Asir 50%	43.3 (42.8; 43.5)	68.3 (68.0; 68.4)	90.9 (90.5; 91.0)	4.8 (4.7; 4.9)	7.4 (7.2; 7.4)	9.8 (9.8; 10.0)
	FBP-Evo	44.2 (43.9; 44.4)	62.4 (61.9; 62.6)	81.1 (80.5; 81.4)	4.9 (4.9; 5.0)	6.9 (6.9; 7.0)	9.0 (8.9; 9.1)
	Asir-V 50%	68.6 (68.1; 68.8)	94.9 (94.2; 95.2)	120.5 (119.6; 120.9)	7.6 (7.6; 7.7)	10.6 (10.5; 10.6)	13.4 (13.3; 13.5)
Philips Healthcare	FBP	49.6 (49.6; 49.7)	77.2 (77.1; 77.2)	98.5 (98.3; 98.9)	5.6 (5.4; 5.6)	8.2 (8.0; 8.3)	11.0 (11.0; 11.1)
	iDose <sup>4</sup> 3	63.9 (63.8; 64.0)	98.9 (98.8; 99.0)	125.1 (124.7; 125.5)	7.1 (7.0; 7.2)	10.4 (10.3; 10.6)	14.0 (14.0; 14.1)
	IMR 2	113.7 (113.4; 113.8)	155.2 (155.0; 155.3)	189.0 (188.4; 189.7)	12.8 (12.8; 12.9)	16.6 (16.5; 16.7)	21.4 (21.3; 21.5)
Siemens Healthineers	FBP-AS+	49.8 (49.7; 50.0)	72.1 (71.9; 72.1)	98.6 (98.5; 98.8)	5.6 (5.5; 5.6)	7.9 (7.9; 8.0)	11.1 (11.0; 11.1)
	SAFIRE 3	73.2 (73.0; 73.3)	108.4 (107.8; 108.6)	146.6 (146.3; 146.8)	8.2 (8.0; 8.2)	12.0 (11.9; 12.0)	16.4 (16.3; 16.5)
	FBP-Edge	53.4 (52.9; 53.6)	81.6 (81.2; 81.7)	100.6 (100.1; 100.7)	5.9 (5.7; 5.9)	9.0 (8.9; 9.0)	11.1 (11.0; 11.2)
	ADMIRE 3	70.9 (70.2; 71.1)	106.9 (106.6; 106.9)	132.9 (132.2; 133)	7.8 (7.7; 7.9)	11.8 (11.7; 11.8)	14.7 (14.6; 14.8)

Note. Values are expressed as median (1st quartile; 3rd quartile). FBP indicates filtered back projection

Manufacturer	Reconstruction type	NPS peak (HU <sup>2</sup> .mm <sup>2</sup> )			NPS spatial frequency (mm <sup>-1</sup> )		
		3 mGy	7 mGy	12 mGy	3 mGy	7 mGy	12 mGy
GE Healthcare	FBP-GSI	897	376	208	0,300	0,310	0,300
	Asir 50%	606	248	143	0,220	0,220	0,220
	FBP-Evo	508	241	151	0,300	0,280	0,300
	Asir-V 50%	298	146	94	0,190	0,170	0,190
Philips Healthcare	FBP	711	294	181	0,200	0,220	0,200
	iDose <sup>4</sup> 3	480	200	128	0,190	0,200	0,190
	IMR 2	103	46	38	0,080	0,090	0,090
Siemens Healthineers	FBP-AS+	611	241	144	0,200	0,220	0,220
	SAFIRE 3	347	130	73	0,170	0,160	0,190
	FBP-Edge	514	235	134	0,200	0,220	0,200
	ADMIRE 3	350	150	89	0,190	0,200	0,200

FBP indicates filtered back projection; NPS indicates noise power spectrum.